BMC Genomics

RESEARCH Open Access

miR-34-5p mediates 20E-induced autophagy in the fat body of *Bombyx mori* by targeting Atg1

Huili Qiao[1*], Ziqian Tong[1], Yuanzhuo Wang[1], Juanjuan Yang[1], Yanyan Sun[1], Huixuan Shi[1], Zhuo Liu[1], Jianping Duan[1], Dandan Li[1] and Yunchao Kan[1,2*]

Abstract

Background 20-Hydroxyecdysone (20E) is an important hormone that regulates insect development and metamorphosis. The fat body of insects plays a crucial role in nutrient storage and energy metabolism and is considered the exchange center for regulating insect development. The fat body undergoes remarkable transformation during insect metamorphosis and is primarily regulated by 20E. microRNAs (miRNAs) have been identified in different insects and have multiple functions in various physiological processes. However, the interaction of 20E and miRNAs in fat body regulation remains unclear.

Results We constructed six small RNA libraries using *Bombyx mori* fat body treated with 20E. Expression and functional analyses were conducted to identify 20E-responsive miRNAs. In total, 431 miRNAs were identified, including 389 known and 42 novel miRNAs. Differential expression analysis revealed significant expression changes in the expression of 40, 9, and 18 miRNAs at 2 h, 6 h, and 12 h after 20E treatment, respectively. The expression of 10 miRNAs was validated using quantitative real-time PCR. *miR-34-5p* is a highly conserved miRNA among the 10 validated miRNAs, and *autophagy-related gene 1* (*Atg1*) was considered a target gene of *miR-34-5p*. The expression analysis of *miR-34-5p* and *Atg1* exhibited an opposite expression pattern in the fat body after the 20E treatment. Dual-luciferase assay indicated that *miR-34-5p* could inhibit *Atg1* expression by targeting a binding site in CDS region of *Atg1*. In larval fat body, overexpressing *miR-34-5p* by injecting *miR-34-5p* agomir suppressed the expression of *Atg1* and autophagy, whereas knocking down *miR-34-5p* by injecting miR-34-5p antagomir induced the expression of *Atg1* and autophagy. Meanwhile, *Atg1* silencing by RNAi also inhibited autophagy. These results indicate that *miR-34-5p* participates in 20E-induced autophagy in *B. mori* fat body by interacting with *Atg1*.

Conclusions We systematically identified and functionally characterized miRNAs associated with 20E regulation in the fat body of *B. mori*. *miR-34-5p* is involved in 20E-induced autophagy in *B. mori* by regulating its target gene *Atg1*. These results provide insight into the role of sophisticated interactions between miRNAs, 20E regulation, and autophagy in fat body remodeling and insect metamorphosis.

*Correspondence:
Huili Qiao
qiaohuili@nynu.edu.cn
Yunchao Kan
kanyunchao@163.com

Full list of author information is available at the end of the article

© The Author(s) 2025. **Open Access** This article is licensed under a Creative Commons Attribution-NonCommercial-NoDerivatives 4.0 International License, which permits any non-commercial use, sharing, distribution and reproduction in any medium or format, as long as you give appropriate credit to the original author(s) and the source, provide a link to the Creative Commons licence, and indicate if you modified the licensed material. You do not have permission under this licence to share adapted material derived from this article or parts of it. The images or other third party material in this article are included in the article's Creative Commons licence, unless indicated otherwise in a credit line to the material. If material is not included in the article's Creative Commons licence and your intended use is not permitted by statutory regulation or exceeds the permitted use, you will need to obtain permission directly from the copyright holder. To view a copy of this licence, visit http://creativecommons.org/licenses/by-nc-nd/4.0/.

Keywords MiRNAs, 20-hydroxyecdysone, Fat body, Autophagy, Metamorphosis

Background

The life cycle of holometabolous insects comprises four distinct stages: egg, larva, pupa, and adult. Two major hormones, juvenile hormone (JH) and 20-hydroxyecdysone (20E), coordinately regulate insect growth and development [1, 2]. The steroid hormone 20E plays an important role during major developmental transitions, including molting and metamorphosis. JH inhibits 20E activity by preventing metamorphosis during the middle larval stages [3, 4]. 20E binds to a nuclear hormone receptor complex formed by the ecdysone receptor (EcR) and ultraspiracle protein (USP) to activate the transcription of early response genes, including *E74,E75,E93*, and *BrC*, which upregulated the expression of late response genes [5, 6]. In addition to these conventional coding genes, noncoding RNAs, particularly microRNAs (miRNAs), are involved in the regulation of the ecdysone signaling pathway and further control the growth and development in insects.

miRNAs are a class of endogenous small noncoding RNAs with a length of 20–25 nucleotides. They are ubiquitous in animals, plants, nematodes, viruses, and other organisms and are highly conserved among species [7]. Usually, miRNAs are initially transcribed from the genome by RNA polymerase II and cleaved into pre-miRNAs by the Drosha complex in the nucleus. Pre-miRNAs are subsequently transported to the cytoplasm and processed into mature miRNAs by Dicer [8]. Finally, they bind to target sites in the 5′-untranslated region (UTR), coding sequence (CDS), or 3′-UTR regions of mRNA, which regulates translational repression or mRNA degradation at the posttranscription level [9, 10]. The development of high-throughput sequencing technology has enabled the identification of miRNAs in various eukaryotic organisms. In mammals, miRNAs predictably control the activities of approximately 50% of all protein-coding genes [11]. miRNAs are involved in many biological processes, such as cell proliferation, differentiation [12], apoptosis [13], autophagy [14], immunity [15], development, and metabolism [16].

To date, miRNAs have been identified in various insects, and studies have indicated that 20E affects miRNA expression. In *Drosophila*, the expression of the let-7 complex, including let-7, miR-100, and miR-125, is induced in S2 cells following the 20E treatment, whereas miR-8, miR-14, and miR-34 expression is inhibited [17–19]. Moreover, the expression of miR-318 is activated by the ecdysone during *Drosophila* oogenesis [20]. In *Blattella germanica*, the expression of let-7, miR-100, and miR-125 are increased after 20E treatment, and miR-252-3p is the only miRNA inhibited by 20E [21]. In *Helicoverpa zea*, the expression of miR-277-3p is downregulated by 20E exposure [22]. In *Galeruca daurica*, 21 and 31 miRNAs were up- and downregulated, respectively, following the 20E treatment [23]. Several miRNAs have been identified and characterized in *Bombyx mori* [24], however, the role of miRNAs in fat body remodeling regulated by 20E remains unclear in many insects.

As a representative economic insect of Lepidoptera, *B. mori* is a useful model for studying the interaction between miRNAs and ecdysone signaling in the fat body. Previous reports show that 20E upregulates autophagy-related genes *(Atgs)* and induces autophagy of the larval fat body in *B. mori* [25, 26]. Herein, miRNAs associated with 20E regulation in the fat body of *B. mori* were identified using small RNA-seq technology. The functions of the putative target genes of the 20E-responsive miRNAs were determined, and the results provide a basis for exploring the regulatory mechanisms of miRNAs in response to 20E in the fat body of *B. mori*.

Methods

Insect rearing and sample collection

A population of silkworm strain Dazao p50 was reared on fresh mulberry leaves at 25℃ under 12 h light/12 h dark cycles. 20E treatment was performed according to a previous study [26]. 2 mg of 20E (Solarbio, China, SE8010) was dissolved in 100 μL of ethanol, and then diluted with sterilized water to 1 mL. The 20E levels in the 2-day-old 5th instar larvae (L5D2) are low, and the fat body is sensitive to 20E [25]. Accordingly, insects at this stage of development were chosen for injection of 20E. The glass pipettes were prepared using two-stage pull method (70℃ for step1 and 60℃ for step 2) with G-100 thin-walled glass capillary using the Model PC-10 puller (NARISHIGE, Japan). For each injection, 2.5 μL (5 μg) aliquots of 20E was aspirated using the prepared glass pipette connected with a CellTram Oil manual microinjector (Eppendorf AG, Germany). After surface sterilization of L5D2 with 75% alcohol, the glass pipette containing 20E was punctured into the intersegmental membrane between the third and fourth abdomen, then 20E was injected directly into the hemolymph. The same volume of solvent was injected as a control.

For small RNA (sRNA) sequencing, fat body tissues from the abdominal segment of the 20E treated and control larvae were separated by forceps and washed with PBS (pH 7.0, 0.1 M), six fat body samples were collected at 2 h, 6 h, and 12 h after injection for both 20E treated groups (named as T_2, T_6, and T_12) and the control groups (named as C_2, C_6, and C_12). For expression analysis, the 5th instar larvae tissues (head, epidermis,

hemolymph, midgut, Malpighian tubules, fat body, silk gland, testis, and ovary) were collected at 24 h after 20E injection, and the midgut were collected after discarding the food residues. Three biological replicates of each samples were collected and frozen immediately in liquid nitrogen and stored at − 80℃ until use.

Total RNA extraction and small RNA sequencing

Total RNA was extracted from each sample using Trizol reagent based on the manufacturer's instructions (Invitrogen, CA, USA). RNA quantitation and quality assessment were conducted at the Novogene Bioinformatics Institute (Beijing, China) following standard procedures. RNA degradation and contamination were monitored on 1% agarose gels. RNA purity was checked using NanoPhotometer spectrophotometer (IMPLEN, CA, USA). RNA concentration was measured using Qubit RNA Assay Kit in Qubit 2.0 Fluorometer (Life Technologies, CA, USA). RNA integrity was assessed using Agilent Bioanalyzer 2100 system (Agilent Technologies, CA, USA).

sRNA separation, library construction, and Illumina sequencing were conducted by the Novogene Bioinformatics Institute (Beijing, China). Total RNA (3 μg) was used as input material for preparing small RNA libraries. Sequencing libraries were generated using NEB Next Multiplex Small RNA Library Prep Set for Illumina (NEB, USA) following the manufacturer's instructions, and index codes were added to attribute sequences to each sample. Briefly, the NEB 3′ SR adaptor was directly and specifically ligated to the 3′ end of miRNA, siRNA, and piRNA. Subsequently, SR RT Primer was hybridized to the excess 3′ SR adaptor that remained free after the 3′ ligation reaction, and a single-stranded DNA adaptor was transformed into a double-stranded DNA molecule. The 5′ ends of the adapter were ligated to those of the miRNA, siRNA, and piRNA molecules. First-strand cDNA was synthesized using M-MuLV Reverse Transcriptase. PCR amplification was performed using LongAmp Taq 2x Master Mix, SR Primer for Illumina, and an index (X) primer. PCR products were purified on an 8% polyacrylamide gel. DNA fragments corresponding to 140–160 bp (the length of small noncoding RNA plus the 3′ and 5′ adaptors) were recovered and dissolved in 8 μL of elution buffer. The library quality was assessed on Agilent Bioanalyzer 2100 system using DNA High Sensitivity Chips. The clustering of the index-coded samples was performed on cBot Cluster Generation System using TruSeq SR Cluster Kit v3-cBot-HS (Illumina) following the manufacturer's instructions. After the cluster generation, libraries were sequenced on Illumina Hiseq 2500/2000 platform and 50 bp single-end reads were generated.

Data assembly and filtration

Raw read data in FASTQ format were processed using custom Perl and Python scripts. Clean data were obtained by removing reads containing ploy-N, with a 5′ adapter, without a 3′ adapter or the insert tag, and low-quality reads from the raw data. The Q20, Q30, and GC contents of the raw data were calculated. The downstream analyses were based on clean, high-quality reads. Reference genomes for *B. mori* were downloaded from SilkDB (http://silkworm.genomics.org.cn/) and NCBI genome (https://www.ncbi.nlm.nih.gov/genome/). The small RNA tags were mapped to the reference sequence using Bowtie [27] without mismatches to analyze the expression and distribution on the reference.

Identification of MiRNAs in B. mori

Known miRNAs were identified based on standard procedure. Briefly, all the known insect miRNAs were downloaded from miRBase v20 (http://www.mirbase.org/). Mapped small RNA tags were used to search for known miRNAs. Modified software mirdeep2 [28] and srnatools-cli were used to obtain potential miRNAs and draw secondary structures. The characteristics of the hairpin structure of the miRNA precursor can be used to predict novel miRNAs. miREvo [29] and miRdeep2 [28] were integrated to predict novel miRNAs by examining the secondary structure, Dicer cleavage site, and minimum free energy of the unannotated small RNA tags. Custom scripts were used to obtain the identified miRNA counts and base bias at the first position with a certain length and on each position of all identified miRNAs. The miRNA families were identified using miFam.dat (http://www.mirbase.org/ftp.shtml) for known miRNAs, and novel miRNA precursors were submitted to Rfam (http://rfam.sanger.ac.uk/search/) to search for Rfam families.

Expression analysis of MiRNAs

The expression profile of miRNAs was analyzed based on an earlier method [30], and the relative expression levels were denoted as transcripts per million (TPM). Differential expression analysis of two groups was performed using DESeq R [31]. *P*-values were adjusted using *q*-values [32]. A q-value < 0.01 and $|\log_2(\text{fold-change})| > 1$ was set as the threshold for significant differential expression analysis.

Target prediction and functional annotation

To further predict the target genes, miRanda [33] was used for miRNA target prediction. Subsequently, the Gene Ontology (GO) and Kyoto Encyclopedia of Genes and Genomes (KEGG) enrichment analyses were applied to obtain annotation information on the functions of the differentially expressed miRNAs and target genes [34–36].

Quantitative real-time PCR

Total RNA was isolated using Trizol reagent (Invitrogen, CA, USA) from the silkworm fat body samples of C_2, T_2, C_6, T_6, C_12, T_12, and the 3-day-old 5th instar larvae tissues (head, epidermis, hemolymph, midgut, Malpighian tubules, fat body, silk gland, testis, and ovary) at 24 h after 20E injection. The expression of the selected miRNAs was measured by quantitative real-time PCR (qRT-PCR). RNA (1 μg) was reverse-transcribed into complementary DNA (cDNA) using a universal adapter primer provided in the All-in-one™ miRNA qRT-PCR Detection Kit (GeneCopoeia, USA, QP115). A miRNA-specific forward primer and a universal RT-PCR primer (complementary to the universal adapter) were used for qRT-PCR following the manufacturer's instructions. qRT-PCR reactions were performed in a 10 μL volume, including 5 μL of 2× All-in-one qPCR mix, 1 μL of miRNA-specific primer (2 μM), 1 μL of universal RT-PCR primer (2 μM), 0.2 μL of ROX reference dye (30 μM), and 1 μL of diluted cDNA. The PCR reactions were incubated at 95℃ for 5 min, followed by 40 cycles of 95℃ for 10 s, 55℃ for 20 s, and 72℃ for 10 s. The 5 S rRNA (GenBank No. M35394.1) was used as a reference sRNA. qRT-PCR was performed on a Bio-Rad CFX96 Real-time PCR Detection System in triplicate. For quantitation of target genes, cDNA was synthesized from 1 μg of total RNA with oligo-dT primer using RevertAid First-Strand cDNA Synthesis Kit (Thermo Fisher, USA, K1622). qRT-PCR reactions were performed in a 10 L volume, which included 5 μL of 2× FastStart Universal SYBR Green Master (ROX) (Roche, Switzerland), 0.3 μL of each gene-specific primer (10 μM), and 1 μL of diluted cDNA. PCR reactions were incubated at 95℃ for 5 min, followed by 40 cycles of 95℃ for 15 s, 55℃ for 30 s, and 72℃ for 30 s. Silkworm *actinA3* (GenBank No. U49854) was used as a reference gene. All primers were designed using the NCBI online primer design tool (https://www.ncbi.nlm.nih.gov/tools/primer-blast/) (Table S1).

Cell transfection and dual-luciferase reporter assay

The partial CDS sequnence (820 ~ 1158) of *Atg1* (GenBank No. XM_012695474.1) was amplified using gene-specific primers (Table S1). *Xho* I and *Not* I restriction enzyme sites were added to the 5′ ends of the forward and reverse primers, respectively. Next, the PCR fragment was cloned into the psiCHECK2 vector (Promega, USA) downstream of the *Renilla* luciferase gene. The gene sequence was confirmed by sequencing at the Beijing Genomics Institute (Shenzhen, China).

Human embryonic kidney 293T (HEK293T) cells were cultured in Dulbecco's modified Eagle's medium (Solarbio, China, 12110) containing 10% fetal bovine serum (Hyclone, USA, SV30087) at 37℃ in a 5% CO_2 atmosphere. The *miR-34-5p* mimics, *miR-34-5p* mutant (mutation in the interaction site at position 2 ~ 8 of miR-34-5p), and miR-NC were synthesized by GenePharma (Suzhou, China) based on the sequences listed in Table S1. HEK293T cells were seeded into 24-well plates with 500 μL cell culture media. Cell transfection was performed once the cells reached 80–90% confluency using X-tremeGENE siRNA transfection reagent per the manufacturer's instructions (Roche, Switzerland, 04476093001). The final concentration of miRNA was 100 nM, and the amount of *Atg1*/psiCHECK2 plasmid in each well was 100 ng. Luciferase activity was measured at 48 h based on the manufacturer's instructions of Dual-Luciferase Reporter Assay System (Promega, USA, E1910). The psiCHECK2 vector contained the *Firefly* and *Renilla* luciferase genes. First, the growth medium was removed from the 24-well plates and cells were washed gently with 500 μL volume of PBS to remove detached cells and residual growth medium. Second, 100 μL of 1x Passive Lysis Buffer was added into per each culture well and the plates were rocked at room temperature for 15 min. Third, 20 μL of cell lysate from each well was carefully transfered into the 96-well ELISA plate containing 100 μL of Luciferase Assay Reagent II, mixed by pipetting 2 or 3 times, and placed the plate in the luminometer to measure the Firefly luciferase activity (Fluc), then 100 μL of Stop & Glo Reagent was added into each well and mixed briefly, the Renilla luciferase activity (Rluc) was measured again. Rluc was normalized to Fluc activity, and the ratio was designated as the relative luciferase activity of each test group. Three biological replicates were performed for each experimental group.

MiRNA and DsRNA injection

The 2-day-old 5th instar larvae were synchronized after molting, and 5 μg of miRNA agomir or antagomir (antisense of agomir with cholesterol modification at the 3′ end, two thioskeleton modifications at the 5′ end, four thioskeleton modifications at the 3′ end, and full chain methoxy modification) for each insect was injected into the hemolymph using the same method as 20E injection. The larvae were dissected at 24 h after injection. Total RNA was extracted from the fat body using Trizol reagent (Invitrogen, CA, USA), and the separated fat body from three individuals was used for LysoTracker Red staining immediately.

For the *Atg1* and *GFP* transcripts, double-stranded RNAs (dsRNA) were designed and synthesized in vitro using T7 RiboMAX™ Express RNAi system (Promega, P1700) based on the manufacturer's instructions. dsAtg1 and dsGFP were analyzed on a 2% agarose gel to confirm their integrity. Next, 10 μg dsRNA was injected into the hemolymph of L5D2 using the same method as 20E injection. The fat body from at least three larvae was

collected and used for qRT-PCR analysis or LysoTracker Red staining at 24 h after injection.

LysoTracker red staining

Following a previously described procedure [26, 37], the larval fat body tissues were collected and fragmented with forceps. They were washed with PBS and stained with LysoTracker Red DND-99 (Thermo Fisher Scientific, L7528) at a final concentration of 50 nM for 5 min at 37℃. After washing three times with PBS, fluorescence observation was done using a Nikon Eclipse C1 confocal microscope.

Statistical analysis

Data were analyzed using Prism 5 software and presented as the mean ± standard error (SE). Figures were prepared using Prism 5 and Adobe Illustrator CS5. The qRT-PCR data were analyzed using two-tailed, unpaired *t*-tests, $^{*}P<0.05$, $^{**}P<0.01$, $^{***}P<0.001$. The statistical significance of the luciferase activity was analyzed using one-way analysis of variance followed by Tukey's test for multiple comparisons. The values are shown as the mean ± SE of three independent experiments. All experiments were repeated three times.

Results

Data analysis of small RNA sequencing

To identify miRNAs in response to the 20E treatment of *B. mori*, six libraries from fat bodies of C_2, T_2, C_6, T_6, C_12, T_12 were constructed and sequenced using Illumina Hiseq. Raw data were deposited in the National Center for Biotechnology Information (NCBI) Short Read Archive under BioProject ID PRJNA1121082. Approximately 7.1–11.2 million raw reads were generated for each sample. After discarding the low-quality reads and adaptor sequences, 6.95–10.95 million clean reads per sample were filtered (Table S2). A total of 81.84–89.75% clean reads were classified as sRNAs with 18–35 nt lengths. The length distribution of the sRNA reads revealed a major peak at 22 nt, which is typical for the distribution of mature miRNAs (Fig. S1). Finally, 89.23–91.75% of the sRNAs were mapped to the silkworm genome (Table S3).

Identification of known and novel MiRNAs

After filtering the dataset and comparing it with known mature miRNAs and miRNA precursors in the miRBase V20 (http://www.mirbase.org/) using the BLAST progr am, we identified 389 mature miRNAs and 406 miRNA precursors. Samples from C_2, T_2, C_6, T_6, C_12, and T_12 yielded 340, 326, 307, 331, 284, and 301 known miRNAs, respectively (Table S4). Using miREvo and mirdeep2 software, we identified miRNAs that did not map to conserved known miRNAs, including 42 novel miRNAs and 43 novel miRNA precursors. Among the six samples, 37, 38, 37, 37, 31, and 36 novel miRNAs were identified (Table S5).

Identification of differentially expressed MiRNAs

Differential expression of miRNAs (DEMs) between the 20E treatment and control was determined based on the normalized differences between Illumina read counts. In total, 40 miRNAs (17 and 23 up- and downregulated) in the T_2 vs. C_2 group, 9 miRNAs (6 and 3 up- and downregulated) in the T_6 vs. C_6 group, and 18 miRNAs (10 and 8 up- and downregulated) in the T_12 vs. C_12 group were significantly, differentially expressed (Fig. 1; Table 1).

Target prediction and functional analysis

To better understand the functions of DEMs in response to 20E, putative DEM target genes were predicted using miRanda. In total, 6005 target genes associated with 12,025 target sites were identified. The predicted target genes for these DEMs were subjected to GO and KEGG enrichment analysis. The GO analysis revealed that the 5667 predicted target genes were enriched in 3626 GO level 2 terms, and 212 GO terms were significantly enriched ($P<0.05$) in the T_2 vs. C_2 group. The GO term types included 110 Biological Process (BB), 20 Cellular Component (CC), and 82 Molecular Function (MF). In the T_6 vs. C_6 group, 2487 predicted target genes were enriched in 2778 GO terms, whereas 51 GO terms were significantly enriched ($P<0.05$), including 13 BB, 2 CC, and 36 MF. In the T_12 vs. C_12 group, 3877 predicted target genes were enriched in 3291 GO terms, and 94 GO terms were significantly enriched ($P<0.05$), including 32 BB, 7 CC, and 55 MF (Table S6). The top 20 terms for each type are presented in Fig. 2.

KEGG analysis revealed that 115 pathways were enriched in the T_2 vs. C_2 group, whereas 114 and 115 pathways were enriched in the T_6 vs. C_6 and T_12 vs. C_12 groups, respectively. The top enriched pathways included "ECM-receptor interaction," "Nucleotide excision repair," and "ABC transporters." "Fatty acid biosynthesis," "Lysine degradation," "Phagosome," and "Inositol phosphate metabolism" were common among the top 20 enriched pathways/processes (Table S7-S9, Fig. S2-S4).

Validation and detection of DEMs and predicted target genes

Because we were interested in miRNAs involved in 20E-regulated autophagy, the target genes of all DEMs were predicted. Then 10 DEMs among the 40 miRNAs in the T_2 vs. C_2 group were selected for validaiton, and they had at least one target gene that was autophagy related genes, 20E receptor genes or 20E-induced genes. 10 DEMs for qRT-PCR analysis included 4 upregulated

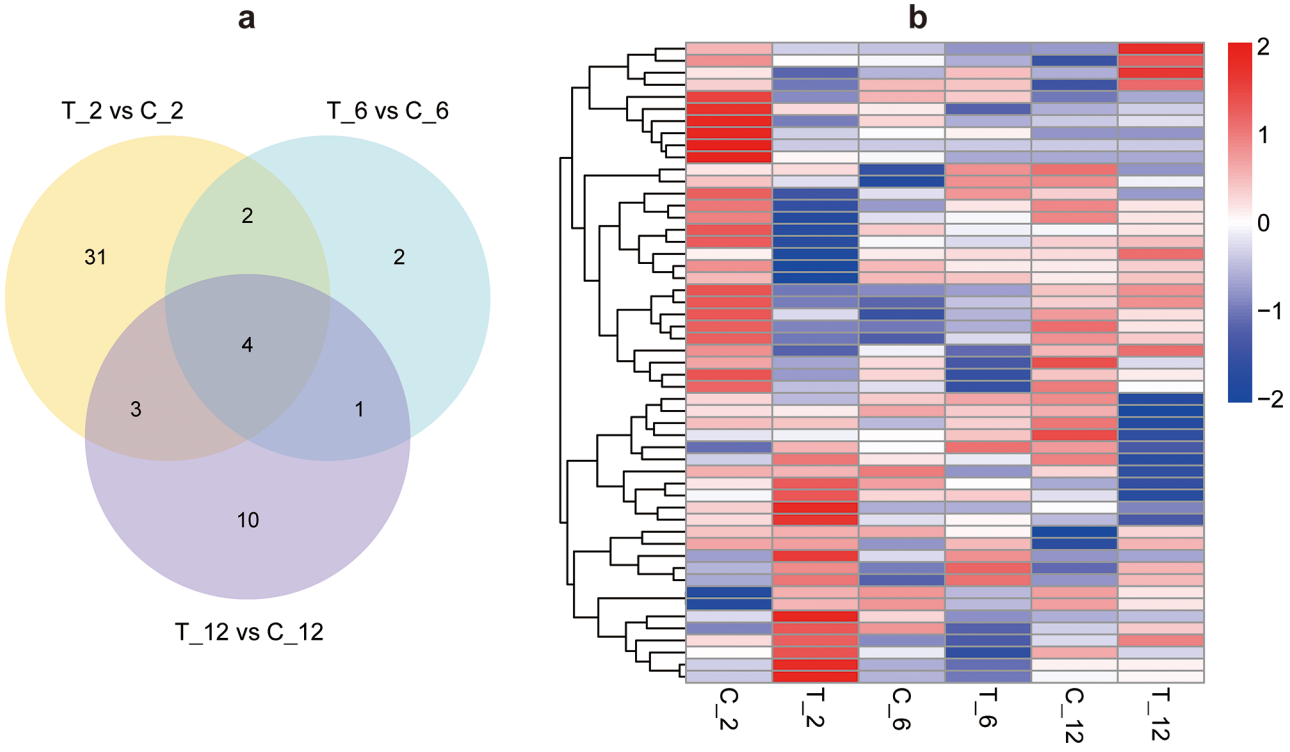

Fig. 1 Venn diagram **(a)** and hierarchical cluster analysis **(b)** of differentially expressed microRNAs in T_2 vs. C_2, T_6 vs. C_6, and T_12 vs. C_12

Table 1 Number of differentially expressed MicroRNAs in each group

DEMs	T_2 vs. C_2	T_6 vs. C_6	T_12 vs. C_12
total	40	9	18
upregulated	17	6	10
downregulated	23	3	8

(*miR-305-5p,miR-275-3p,miR-34-5p*, and *miR-282-5p*) and 6 downregulated (*miR-281-3p,miR-375-3p,miR-274-5p,miR-3220,miR-3244*, and *novel-46*) miRNAs. The results showed that all 10 miRNAs exhibited similar expression patterns compared with those analyzed by RNA sequencing (Fig. 3).

Upregulated *miR-34-5p* and downregulated *miR-281-3p*, which exhibited the highest fold-change, were selected for further expression analysis in the fat bodies of C_2, T_2, C_6, T_6, C_12, T_12. *miR-34-5p* was significantly upregulated in T_2 compared with C_2 but was significantly downregulated in T_6 and T_12 (Fig. 4a). Compared with the control, *miR-281-3p* was significantly down- and upregulated in T_2 and T_12, respectively, but not significantly different in T_6 (Fig. 4b).

Based on the target gene prediction results, *miR-34-5p* and *miR-281-3p* had 366 and 371 predicted target genes, respectively. *miR-281-3p* has been reported to participate in *B. mori* developmental regulation in the Malpighian tubule through the suppression of the *EcRB* expression [38]. As one of the predicted target genes of *miR-34-5p,Atg1* is required for autophagosome initiation and is sensitive to 20E injection. To clarify the function of *miR-34-5p* in 20E regulated autophagy and fat body development, we focused on *miR-34-5p* and *Atg1* in the following experiments. In contrast with *miR-34-5p,Atg1* expression was significantly downregulated at 2 h after 20E injection compared with the control and significantly upregulated at 6 h and 12 h after 20E injeciton (Fig. 4c).

Furthermore, we analyzed the expression of *miR-34-5p* and *Atg1* in different tissues of silkworm larvae. The expression of *miR-34-5p* in the control group was the highest in hemolymph, the lowest in midgut and silk gland, and low in other tissues, respectively. After a 24 h 20E exposure, *miR-34-5p* was significantly decreased in hemolymph, fat body, and testis, but increased in head, epidermis, Malpighian, and ovary (Fig. 5a). *Atg1* expression in the control group was relatively high in testis, ovary, head, epidermis, and silk gland, whereas it was the lowest in hemolymph. In the 20E treatment group, *Atg1* was significantly increased in epidermis, Malpighian, and fat body, but decreased in midgut, silk gland, and ovary (Fig. 5b). Although the trend in *miR-34-5p* and *Atg1* expression was different, they still exhibited opposite expression patterns in the fat body after the 20E treatment.

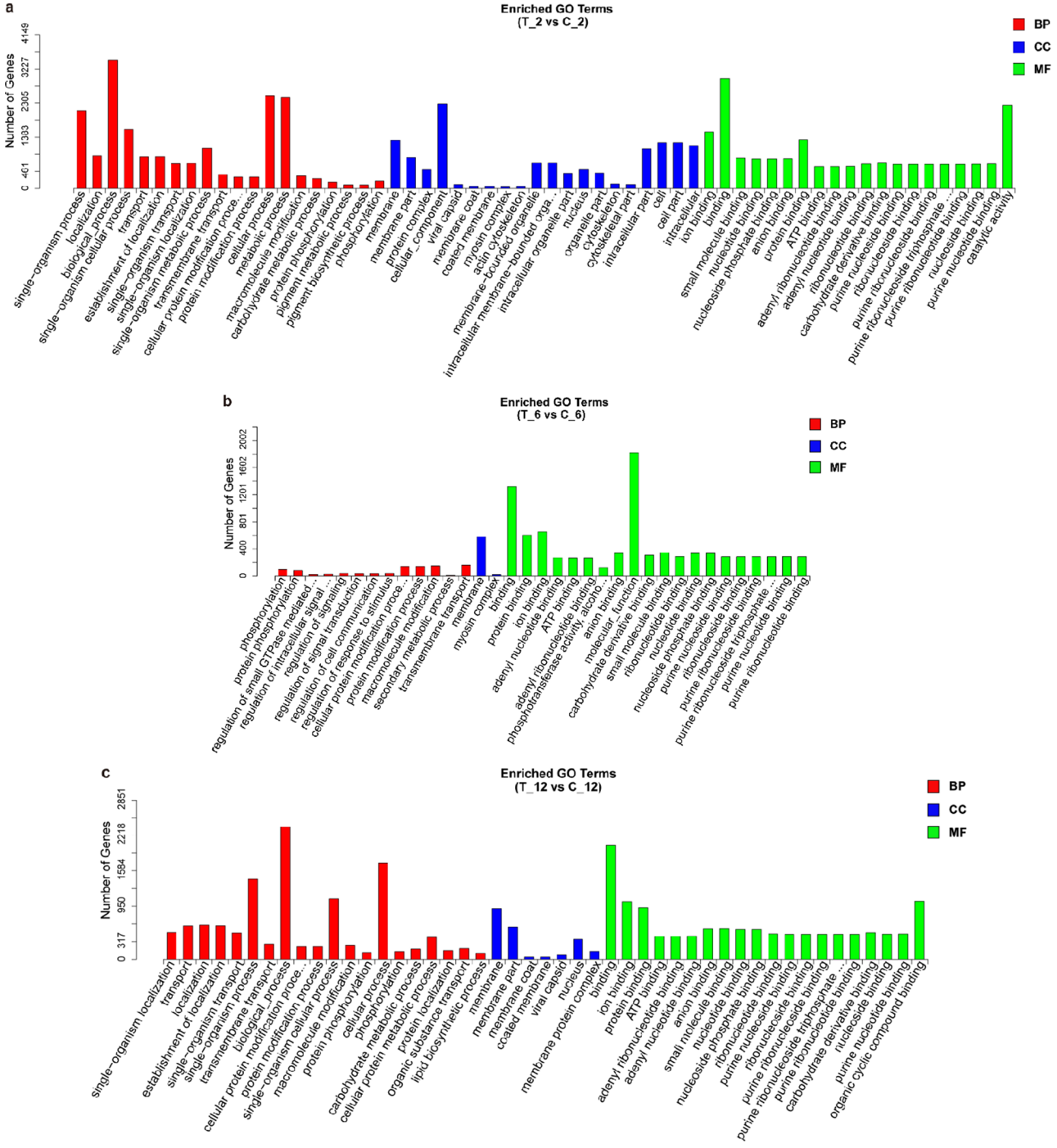

Fig. 2 Histogram of Gene Ontology enrichment for putative target genes of differentially expressed microRNAs in T_2 vs. C_2 **(a)**, T_6 vs. C_6 **(b)**, and T_12 vs. C_12 **(c)**

In vitro validation of miR-34-5p target gene

An interaction site analysis of *miR-34-5p* and *Atg1* revealed that *miR-34-5p* targets a CDS region of *Atg1* (Fig. 6a), suggesting that *Atg1* is a potential target of *miR-34-5p*. To confirm the interaction between *miR-34-5p* and *Atg1*, we introduced the partial CDS sequence of *Atg1* at the downstream of the *Renilla* luciferase gene in the psiCHECK2 vector. *miR-34-5p* mutant was the RNA oligomer mutated in the interaction site at position 2 ~ 8 of *miR-34-5p*. For high transfection efficiency and low background expression of *miR-34-5p*, HEK293T cell line was used for Dual luciferase reporter assay. *Atg1*/psiCHECK2 were transfected into HEK293T cells with the mimics, mutant and negative control of *miR-34-5p*.

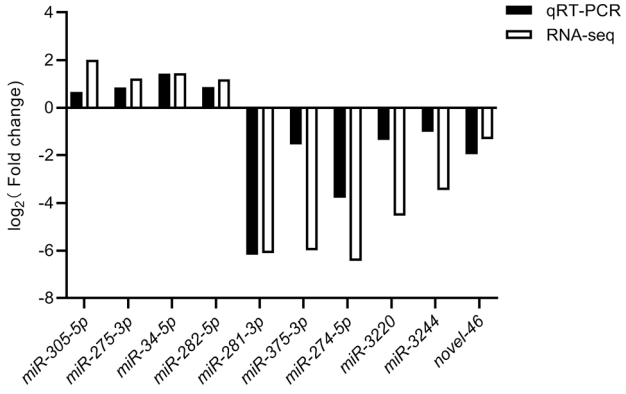

Fig. 3 Validation of small RNA sequencing changes in transcript abundance as measured by qRT-PCR for 10 differentially expressed miRNAs in T_2 vs. C_2 group. qRT-PCR of each miRNA were performed in three replicates of C_2 or T_2 samples. Fold-change: normalization values in the small RNA sequencing data and the mean of three relative expression values obtained with qRT-PCR based on the $2^{-\Delta\Delta Ct}$ method

The luciferase activity was significantly reduced to 56% in the presence of *miR-34-5p* mimics compared with the vector control. Mutation of *miR-34-5p* abolished the suppression effect on the reporter activity of the *Atg1* target site (Fig. 6b). The results indicated that *Atg1* is the target gene of *miR-34-5p*, and *miR-34-5p* can silence *Atg1* expression via targeting the CDS region of *Atg1*.

Overexpression and Inhibition of miR-34-5p in vivo

Atg1 plays an important role in initiating autophagy. To determine the relationship between *miR-34-5p* and autophagy, a *miR-34-5p* agomir and antagomir were injected separately into L5D2 larvae and the expression of *miR-34-5p* and *Atg1* was analyzed in the fat body. Compared with the agomir NC, *miR-34-5p* expression was significantly increased after agomir injection (Fig. 7a); however, the expression of *Atg1* was decreased (Fig. 7b). By contrast, the *miR-34-5p* antagomir significantly decreased the *miR-34-5p* expression (Fig. 7c) and increased the *Atg1* expression compared with the antagomir NC (Fig. 7d). These results indicate that *miR-34-5p* can be successfully overexpressed or inhibited in the fat body of the silkworm, and the expression pattern of *miR-34-5p* and *Atg1* was opposite of one another.

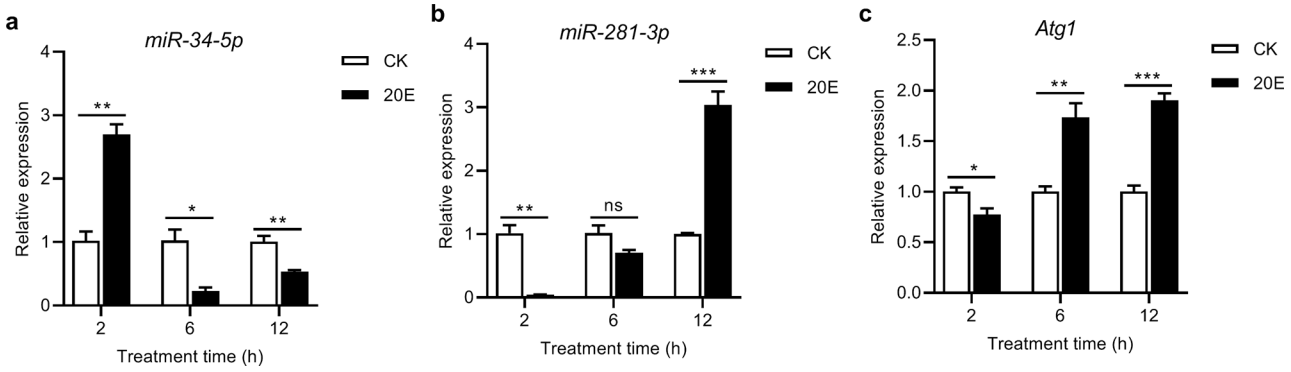

Fig. 4 Expression profile of miR-34-5p **(a)**, miR-281-3p **(b)**, and *Atg1***(c)** in the 20E-treated fat body of *Bombyx mori* measured by qRT-PCR. Data were normalized to the reference genes 5 S rRNA or *actinA3* and are shown as the mean ± standard error; **P* < 0.05, ***P* < 0.01, ****P* < 0.001; no significant differences are denoted by ns above the bars; two-tailed; unpaired *t-test*

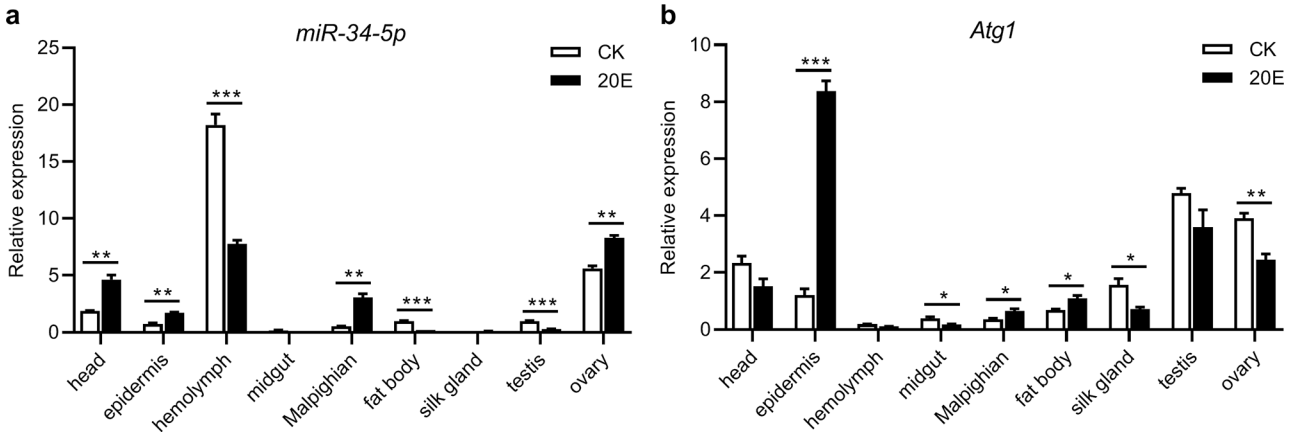

Fig. 5 Expression profile of *miR-34-5p***(a)** and *Atg1***(b)** in different tissues of 5th instar larvae of *Bombyx mori* measured by qRT-PCR; data were normalized to the reference genes 5 S rRNA or *actinA3* and are shown as the mean ± standard error; **P* < 0.05, ***P* < 0.01, ****P* < 0.001; two-tailed; unpaired *t-test*

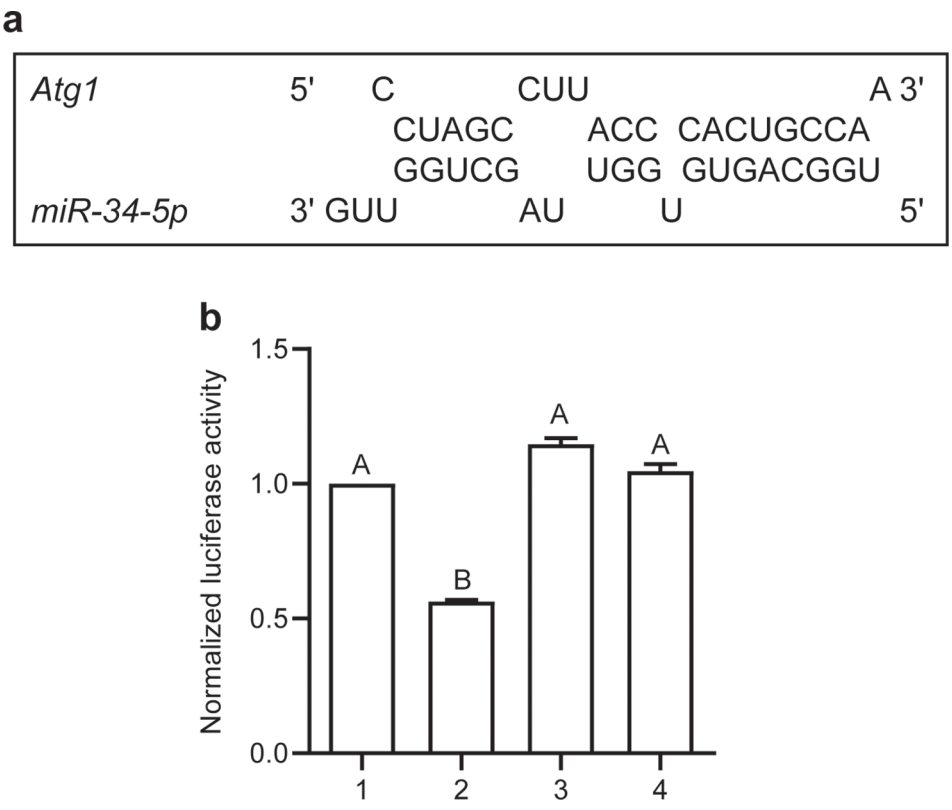

Fig. 6 Target verification of *miR-34-5p*; **(a)** interaction sites of *miR-34-5p* and *Atg1*; **(b)** target verification of *miR-34-5p* by luciferase assay; (1) *Atg1*/psiCHECK2, (2) *Atg1*/psiCHECK2 and *miR-34-5p* mimics, (3) *Atg1*/psiCHECK2 and *miR-34-5p* mutant, and (4) *Atg1*/psiCHECK2 and *miR-34-5p* negative control. Three independent experiments were performed and each sample was repeated three times. Data are shown as the means ± standard error, significant differences are denoted by different letters ($P < 0.01$, one-way analysis of variance, Tukey's multiple comparison test)

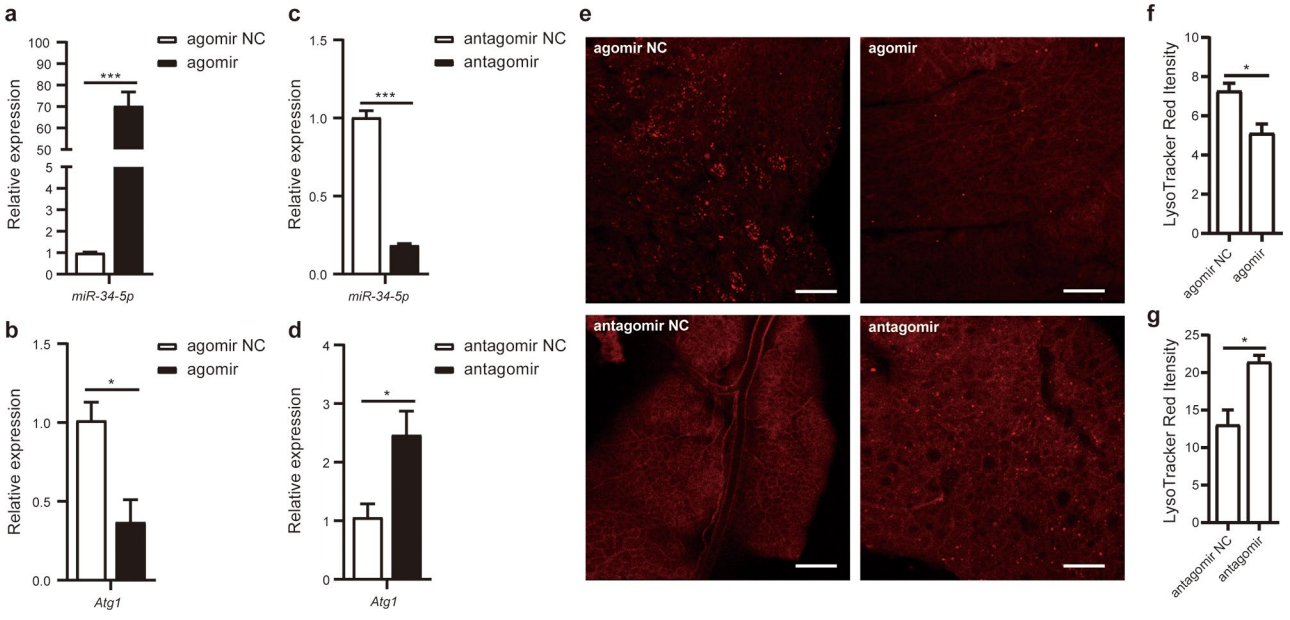

Fig. 7 Autophagy detection in the silkworm fat body. **(a–d)** qRT-PCR measurement of *miR-34-5p* and *Atg1* expression after *miR-34-5p* overexpression or inhibition; **(e–g)** LysoTracker Red staining of the fat body after *miR-34-5p* overexpression or inhibition (red, magnification 40×, the scale is 50 μm)

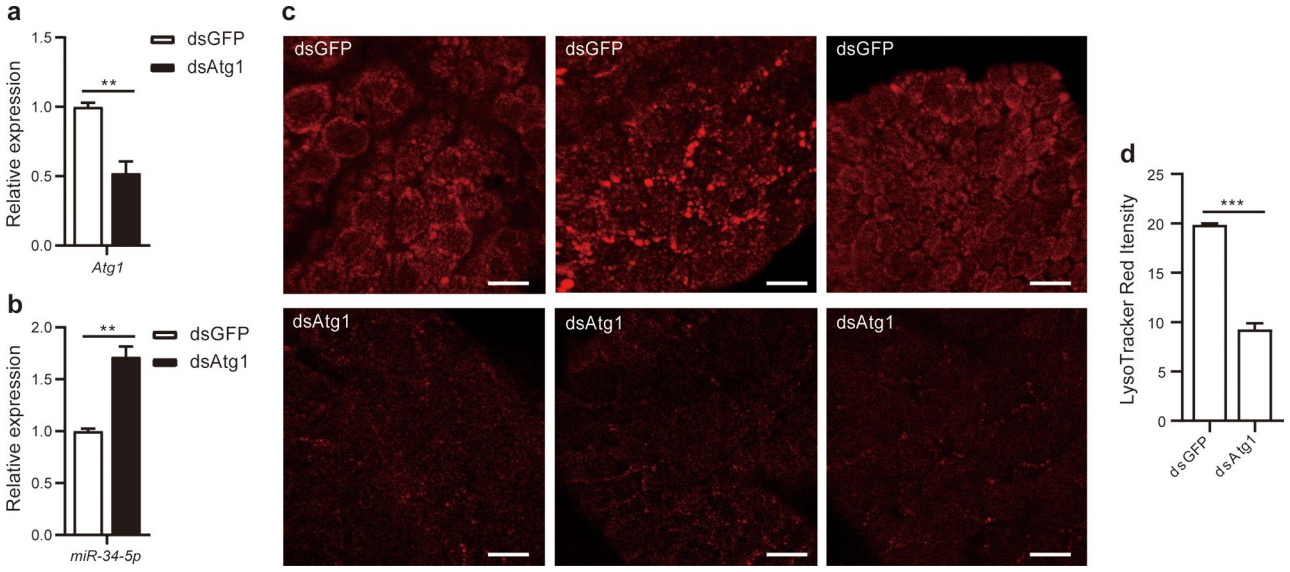

Fig. 8 RNAi of *Atg1* in the silkworm; **(a–b)** qRT-PCR measurement of *Atg1* and *miR-34-5p* in fat body after *Atg1* silencing; **(c–d)** LysoTracker Red staining of fat body after *Atg1* silencing (red, magnification 40×, the scale is 50 μm)

LysoTracker is an acidotropic dye that stains cellular acidic compartments, including lysosomes and autolysosomes. It has been used to detect autophagy-associated lysosomal activity from yeast to human [39, 40]. Using LysoTracker Red staining, the autophagic process in silkworm fat body was monitored. The LysoTracker Red fluorescence intensity was significantly decreased after *miR-34-5p* overexpression compared with that in the agomir NC control, but significantly increased after *miR-34-5p* inhibition compared with that in the antagomir NC control (Fig. 7e-g).

RNA interference of Atg1 in vivo

An RNA interference experiment was performed on *Atg1* in the 5th larvae. A double-stranded RNA targeting *Atg1* was injected into L5D2 larvae. The results of qRT-PCR showed that the Atg1 expression was significantly decreased in dsAtg1-injected fat body compared with the dsGFP control (Fig. 8a), which indicated that the expression of *Atg1* was successfully silenced in larval fat body. Meanwhile, we also found that knockdown of *Atg1* resulted in a significant increase in *miR-34-5p* expression (Fig. 8b). LysoTracker Red staining of the fat body from three replicates was all reduced after injecting dsAtg1 (Fig. 8c) and the fluorescence intensity was significantly decreased after Atg1 silencing (Fig. 8d). These results indicate that *miR-34-5p* inhibits autophagy by regulating its target gene *Atg1*.

Discussion

The insect fat body plays an important role in nutrient storage and energy metabolism and is considered the exchange center for regulating insect development and behavior. The fat body undergoes a remarkable transformation during insect metamorphosis, known as fat body remodeling. This process includes autophagy, apoptosis, cell dissociation of fat body cells during the larval stage, and the formation of new fat body tissue during the adult stage, which is primarily regulated by the steroid hormone 20E [41, 42]. miRNAs regulate insect growth, molting, metamorphosis, innate immunity, and reproduction by interacting with different target genes in multiple hormonal pathways [19, 43–50]. Further, 20E may regulate fat body modeling and insect metamorphosis through miRNAs and their target genes in the ecdysone signaling pathway. Herein, we performed small RNA sequencing and qRT-PCR validation using total RNA extracted from the L5D2 fat body at 2, 6, and 12 h after 20E injection to identify miRNAs involved in 20E regulation in the fat body of *B. mori*. In total, 389 mature miRNAs, 406 miRNA precursors, 42 novel miRNAs, and 43 novel miRNA precursors were identified from various fat body samples. Differential expression analysis yielded 40, 9, and 18 DEMs in the T_2 vs. C_2, T_6 vs. C_6, and T_12 vs. C_12 groups, respectively, after the 20E treatment (Table 1). In *Galeruca daurica*, 52 miRNAs were significantly differentially expressed after 20 treatments [23]. Jin et al. (2020) found 22 and 66 DEMs at 6 h and 6 days following the 20E treatment of the BmE cell line, and 9 and 78 DEMs at 6 and 48 h after the 20E treatment in the *Drosophila* S2 cell line [44]. These results suggest that miRNAs play important roles in hormone regulation pathways.

Although 20E-responsive miRNAs have been extensively studied, the regulatory mechanism between miRNAs and the ecdysone signaling pathway is not well

understood. Following qRT-PCR validation and target prediction, an 20E-responsive miRNA, *miR-34-5p*, and its predicted target gene, *Atg1*, were selected to further clarify its function in 20E regulation. miR-34 is a highly conserved miRNA and plays an important role in various organisms. Atg1 is a serine/threonine protein kinase that has a role in autophagy. 20E induces the expression of most *Atg* genes to initiate autophagy when MTORC1 activity is inhibited in silkworms. Atg1 is indispensable for the initial step of autophagosome formation [25, 51]. We found that *miR-34-5p* and *Atg1* exhibit a time-dependent pattern in response to 20E in the fat body, but their expression changes contrast with one another (Fig. 4). The expression of *miR-34-5p* was downregulated while *Atg1* was upregulated at 6 h and 12 h after 20E injection, which was consistent with previous studies in *B. mori* and *Nilaparvata lugens* [26, 52]. However, *miR-34-5p* was upregulated at 2 h after 20E injection, which opens a new question whether other target genes of *miR-34-5p* are involved in the early 20E regulation, and if so, what is the relationship with 20E regulated autophagy.

miRNAs are well known to selectively target 3'UTRs of mRNA to silence gene expression at post transcriptional levels. However, multiple reports have characterized a number of functional miRNA recognition elements (MREs) in CDS in mammals [53–58]. In this study, we found that *miR-34-5p* targeted a CDS region of *Atg1*. Dual-luciferase reporter assay indicated that the luciferase activity was significantly reduced when *Atg1*/psiCHECK2 and *miR-34-5p* were transfected together (Fig. 6). In mammals, the typical MREs in 3'UTRs lost function when moved it to CDS [59], but some MREs in CDS were functional when placed in 3'UTRs [53–57]. In *Drosophila*, The conserved miR-932 could regulate the expression of *dnlg2* via binding CDS region of *dnlg2*, and the level of DNlg2 as well as its mRNA were decreased by miR-932 [60]. Recently, Zhang et al. (2018) found a class of MREs that exclusively functioned in CDS regions in humans with distinct mechanism [58]. Nevertheless, the mechanism of *miR-34-5p* repressing *Atg1* expression still need further study to reveal.

In *vivo,miR-34-5p* was overexpressed in the L5D2 fat body by injecting an agomir which caused the inhibition of *Atg1* expression and autophagy, whereas *miR-34-5p* inhibition by injecting antagomir induced the expression of *Atg1* and autophagy (Fig. 7). Meanwhile, the expression of *Atg1* was reduced by RNAi and resulted in inhibition of autophagy (Fig. 8). In *Caenorhabditis elegans,miR-34* modulates lifespan by repressing the autophagy gene *Atg9* [61]. In *Drosophila,miR-34* modulates ecdysone signaling by repressing the expression of *Eip74EF,Eip75B*, and *BrC* [48]. In honeybees, *miR-34-5p* regulates the expression of pair-rule and cytoskeleton genes during early development and controls insect segmentation [62]. In *N. lugens,miR-34* mediates crosstalk between the 20E, JH, and IIS pathways and regulates wing polyphenism [52]. In *B. mori,miR-34-5p* controls larval growth and wing morphology by targeting *BmE74* and *BmCPG4* [63]. Therefore, our findings indicate that *miR-34-5p* can regulate *Atg1* expression at both protein and mRNA level. These results showed that *miR-34-5p* participates in the 20E-mediated autophagy of the fat body by interacting with *Atg1* in *B. mori*, which can affect the fat body remodeling required for insect metamorphosis.

We also found that the expression of *miR-34-5p* was increased after silencing *Atg1* by RNAi (Fig. 8b). The internal regulation mechanism behind this result is still unknown, but the studies of *miR-34* in other insects may provide some hints. *miR-34* is maternally inherited in *Drosophila* and activated by JH but is suppressed by 20E through *BrC* [17, 64]. JH has been reported to show antagonistic interaction with 20E through *BrC* [65]. In *Aedes aegypti*, ecdysteroid induced *Atg* expression to initiate autophagy during midgut remodeling, but JH inhibited midgut remodeling during metamorphosis by interfering with the expression of *Atg* genes [66]. In *N. lugens*, knockdown *BrC* by RNAi resulted in the significant increase of *miR-34* at the third instar numphs, while *miR-34* was also downregulated by 20E and upregulated by JH which are likely mediated by *BrC* in a transcriptional regulation manner [52]. Whether the conserved *miR-34-5p* mediates the cross talk between 20E, JH and autophagy pathway by forming a feedback loop in *B.mori* fat body, more research should be conducted to clarify this question.

Conclusions

We constructed six small RNA libraries of *B. mori* fat body to identify miRNAs involved in 20E regulation. A total of 431 miRNAs, including 389 known and 42 novel miRNAs, were identified with 40, 9, and 18 miRNAs differentially expressed at 2, 6, and 12 h after the 20E treatment, of which, 10 were validated by qRT-PCR. A functional study of *miR-34-5p* indicated that *Atg1* was its target gene, and *miR-34-5p* was involved in 20E-induced autophagy by regulating *Atg1*. These results shed light on the interactions between miRNAs, 20E regulation, and autophagy on fat body remodeling and insect metamorphosis.

Abbreviations

miRNA	microRNA
20E	20-hydroxyecdysone
JH	Juvenile hormone
EcR	Ecdysone receptor
USP	Ultraspiracle protein
BrC	Broad complex
UTR	Untranslated region
CDS	Coding sequence
TPM	Transcripts per million
GO	Gene Ontology

KEGG	Kyoto Encyclopedia of Genes and Genomes
DEM	Differentially expressed miRNA
Atg	Autophagy-related gene
MTORC1	mechanistic target of rapamycin complex 1
IIS	Insulin/IGF-1 signaling

Supplementary Information

The online version contains supplementary material available at https://doi.org/10.1186/s12864-025-11499-9.

Supplementary Material 1

Supplementary Material 2

Acknowledgements
We thank Beijing Novogene Technology Co., Ltd for assisting in sequencing and bioinformatic analysis. We thank Muwang Li from the Sericultural Research Institute, Chinese Academy of Agricultural Sciences for providing the Bombyx mori strains. We also thank Yang Cao and Ling Tian from College of Animal Science, South China Agricultural University for their kind suggestions and help in autophagy detection.

Author contributions
YK and HQ conceived and designed the experiment. YK, HQ and JD obtained the research funds. HQ, ZT, YW, JY and YS performed the experiments. HQ, ZT, HS and ZL analyzed all the data. HQ wrote the manuscript. YK, JD and DL assisted in the data analysis and manuscript revision. All of the authors read and approved the final manuscript.

Funding
This research was supported by grants from the National Natural Science Foundation of China (No. 32070503), Key Research and Development Program of Henan Province, China (231111111000), Key Scientific Research Projects of Colleges and Universities in Henan Province, China (24A180020), and Natural Science Foundation of Henan Province, China (232300420022). The funding bodies had no role in the design of the study and collection, analysis, and interpretation of data and in writing the manuscript.

Data availability
The datasets generated during the current study are available in the SRA database of the NCBI system with accession number of PRJNA1121082.

Declarations

Ethics approval and consent to participate
Not applicable.

Consent for publication
Not applicable.

Competing interests
The authors declare no competing interests.

Author details
[1]Henan Key Laboratory of Insect Biology in Funiu Mountain, Henan International Joint Laboratory of Insect Biology, College of Life Science, Nanyang Normal University, Nanyang, Henan 473061, China
[2]School of Resourses and Enviroment, Henan Institute of Science and Technology, Xinxiang, Henan 453003, China

Received: 2 July 2024 / Accepted: 18 March 2025
Published online: 31 March 2025

References

1. Truman JW, Riddiford LM. The origins of insects metamorphosis. Nature. 1999;401(6752):447–52.
2. Dubrovsky EB. Hormonal cross talk in insect development. Trends Endocrinol Metab. 2005;16(1):6–11.
3. Gilbert LI, Rybczynski R, Warren JT. Control and biochemical nature of the ecdysteroidogenic pathway. Annu Rev Entomol. 2002;47:883–916.
4. Riddiford LM. How does juvenile hormone control insect metamorphosis and reproduction? Gen Comp Endocrinol. 2012;179(3):477–84.
5. Riddiford LM, Cherbas P, Truman JW. Ecdysone receptors and their biological actions. Vitam Horm. 2000;60:1–73.
6. Yamanaka N, Rewitz KF, O'Connor MB. Ecdysone control of developmental transitions: lessons from *Drosophila* research. Annu Rev Entomol. 2013;58:497–516.
7. Ambros V. The functions of animal MicroRNAs. Nature. 2004;431(7006):350–5.
8. Kim VN, Han J, Siomi MC. Biogenesis of small RNAs in animals. Nat Rev Mol Cell Biol. 2009;10(2):126–39.
9. Bartel DP, Chen CZ. Micromanagers of gene expression: the potentially widespread influence of metazoan MicroRNAs. Nat Rev Genet. 2004;5(5):396–400.
10. Guo ZW, Xie C, Yang JR, Li JH, Yang JH, Zheng L. MtiBase: a database for decoding MicroRNA target sites located within CDS and 5'UTR regions from CLIP-Seq and expression profile datasets. Database (Oxford). 2015;2015:bav102.
11. Krol J, Loedige I, Filipowicz W. The widespread regulation of MicroRNA biogenesis, function and decay. Nat Rev Gene. 2010;11(9):597–610.
12. Li Y, Wang H, Tao K, Xiao Q, Huang Z, Zhong L, et al. miR-29b suppresses CML cell proliferation and induces apoptosis via regulation of BCR/ABL1 protein. Exp Cell Res. 2013;319(8):1094–101.
13. Li Y, Jiang J, Liu W, Wang H, Zhao L, Liu S, et al. microRNA-378 promotes autophagy and inhibits apoptosis in skeletal muscle. Proc Natl Acad Sci USA. 2018;115(46):E10849–58.
14. Nelson C, Ambros V, Baehrecke EH. miR-14 regulates autophagy during developmental cell death by targeting ip3-kinase 2. Mol Cell. 2014;56(3):376–88.
15. Xu SJ, Hu HT, Li HL, Chang S. The role of MiRNAs in immune cell development, immune cell activation, and tumor immunity: with a focus on macrophages and natural killer cells. Cells. 2019;8(10):1140.
16. Ameres SL, Zamore PD. Diversifying MicroRNA sequence and function. Nat Rev Mol Cell Biol. 2013;14(8):475–88.
17. Sempere LF, Sokol NS, Dubrovsky EB, Berger EM, Ambros V. Temporal regulation of MicroRNA expression in *Drosophila melanogaster* mediated by hormonal signals and broad-Complex gene activity. Dev Biol. 2003;259(1):9–18.
18. Varghese J, Cohen SM. MicroRNA miR-14 acts to modulate a positive autoregulatory loop controlling steroid hormone signaling in *Drosophila*. Genes Dev. 2007;21(18):2277–82.
19. Jin H, Kim VN, Hyun S. Conserved MicroRNA miR-8 controls body size in response to steroid signaling in *Drosophila*. Genes Dev. 2012;26(13):1427–32.
20. Ge W, Deng Q, Guo T, Hong X, Kugler JM, Yang X, et al. Regulation of pattern formation and gene amplification during *Drosophila* oogenesis by the miR-318 MicroRNA. Genetics. 2015;200(1):255–65.
21. Rubio M, de Horna A, Belles X. MicroRNAs in metamorphic and non-metamorphic transitions in Hemimetabolan insect metamorphosis. BMC Genomics. 2012;13:386.
22. Reynolds JA, Nachman RJ, Denlinger DL. Distinct MicroRNA and mRNA responses elicited by ecdysone, diapause hormone and a diapause hormone analog at diapause termination in pupae of the corn earworm, *Helicoverpa Zea*. Gen Comp Endocrinol. 2019;278:68–78.
23. Wang HC, Han HB, Duan TF, Li L, Pang BP. Transcriptome-wide identification of MicroRNAs in response to 20-hydroxyecdysone in *Galeruca Daurica*. Comp Biochem Physiol Part D Genomics Proteom. 2022;42:100981.
24. Wang X, Tang SM, Shen XJ. Overview of research on *Bombyx Mori* MicroRNA. J Insect Sci. 2014;14:133.
25. Tian L, Ma L, Guo E, Deng X, Ma S, Xia Q, et al. 20-Hydroxyecdysone upregulates Atg genes to induce autophagy in the *Bombyx* fat body. Autophagy. 2013;9(8):1172–87.
26. Qiao H, Wang J, Wang Y, Yang J, Wei B, Li M, et al. Transcriptome analysis reveals potential function of long non-coding RNAs in 20-hydroxyecdysone regulated autophagy in *Bombyx Mori*. BMC Genomics. 2021;22(1):374.
27. Langmead B, Trapnell C, Pop M, Salzberg SL. Ultrafast and memory-efficient alignment of short DNA sequences to the human genome. Genome Biol. 2009;10(3):R25.
28. Friedländer MR, Mackowiak SD, Li N, Chen W, Rajewsky N. miRDeep2 accurately identifies known and hundreds of novel MicroRNA genes in seven animal clades. Nucleic Acids Res. 2012;40(1):37–52.

29. Wen M, Shen Y, Shi S, Tang T. MiREvo: an integrative MicroRNA evolutionary analysis platform for next-generation sequencing experiments. BMC Bioinformatics. 2012;13:140.
30. Zhou L, Chen J, Li Z, Li X, Hu X, Huang Y, et al. Integrated profiling of MicroRNAs and mRNAs: MicroRNAs located on Xq27.3 associate with clear cell renal cell carcinoma. PLoS ONE. 2010;5(12):e15224.
31. Wang L, Feng Z, Wang X, Wang X, Zhang X. DEGseq: an R package for identifying differentially expressed genes from RNA-seq data. Bioinformatics. 2010;26(1):136–8.
32. Storey JD. The positive false discovery rate: A bayesian interpretation and the q-value. Ann Stat. 2003;31:2013–35.
33. Enright AJ, John B, Gaul U, Tuschl T, Sander C, Marks DS. MicroRNA targets in *Drosophila*. Genome Biol. 2003;5(1):R1.
34. Young MD, Wakeeld MJ, Smyth GK, Oshlack A. goseq: Gene Ontology testing for RNA-seq datasets. 2012
35. Mao X, Cai T, Olyarchuk JG, Wei L. Automated genome annotation and pathway identification using the KEGG orthology (KO) as a controlled vocabulary. Bioinformatics. 2005;21(19):3787–93.
36. Kanehisa M, Araki M, Goto S, Hattori M, Hirakawa M, Itoh M, et al. KEGG for linking genomes to life and the environment. Nucleic Acids Res. 2008;36(Database issue):D480–4.
37. Xie K, Tian L, Guo X, Li K, Li J, Deng X, et al. BmATG5 and BmATG6 mediate apoptosis following autophagy induced by 20-hydroxyecdysone or starvation. Autophagy. 2016;12(2):381–96.
38. Jiang J, Ge X, Li Z, Wang Y, Song Q, Stanley DW, et al. MicroRNA-281 regulates the expression of ecdysone receptor (EcR) isoform B in the silkworm, *Bombyx Mori*. Insect Biochem Mol Biol. 2013;3(8):692–700.
39. Klionsky DJ, Cuervo AM, Seglen PO. Methods for monitoring autophagy from yeast to human. Autophagy. 2007;3(3):181–206.
40. DeVorkin L, Gorski SM. LysoTracker staining to aid in monitoring autophagy in *Drosophila*. Cold Spring Harb Protoc. 2014;2014(9):951–8.
41. Zheng H, Yang X, Xi Y. Fat body remodeling and homeostasis control in *Drosophila*. Life Sci. 2016;167:22–31.
42. Li S, Yu X, Feng Q. Fat body biology in the last decade. Annu Rev Entomol. 2019;64:315–33.
43. Bryant B, Macdonald W, Raikhel AS. MicroRNA miR-275 is indispensable for blood digestion and egg development in the mosquito *Aedes aegypti*. Proc Natl Acad Sci USA. 2010;107(52):22391–98.
44. Jin X, Wu X, Zhou L, He T, Yin Q, Liu S. 20-Hydroxyecdysone-responsive MicroRNAs of insects. RNA Biol. 2020;17(10):1454–71.
45. Boulan L, Martín D, Milán M. Bantam MiRNA promotes systemic growth by connecting insulin signaling and ecdysone production. Curr Biol. 2013;23(6):473–8.
46. Ling L, Ge X, Li Z, Zeng B, Xu J, Aslam AF, et al. MicroRNA Let-7 regulates molting and metamorphosis in the silkworm, *Bombyx Mori*. Insect Biochem Mol Biol. 2014;53:13–21.
47. Lozano J, Montañez R, Belles X. MiR-2 family regulates insect metamorphosis by controlling the juvenile hormone signaling pathway. Proc Natl Acad Sci USA. 2015;112(12):3740–45.
48. Xiong XP, Kurthkoti K, Chang KY, Li JL, Ren X, Ni JQ, et al. miR-34 modulates innate immunity and ecdysone signaling in *Drosophila*. PLoS Pathog. 2016;12(11):e1006034.
49. Liu Z, Ling L, Xu J, Zeng B, Huang Y, Shang P, et al. MicroRNA-14 regulates larval development time in *Bombyx Mori*. Insect Biochem Mol Biol. 2018;93:57–65.
50. Lee S, Kim N, Jang D, Kim HK, Kim J, Jeon JW, et al. Ecdysone-induced MicroRNA miR-276a-3p controls developmental growth by targeting the insulin-like receptor in *Drosophila*. Insect Mol Biol. 2023;32(6):703–15.
51. Casati B, Terova G, Cattaneo AG, Rimoldi S, Franzetti E, de Eguileor M, et al. Molecular cloning, characterization and expression analysis of ATG1 in the silkworm, *Bombyx Mori*. Gene. 2012;511(2):326–37.
52. Ye X, Xu L, Li X, He K, Hua H, Cao Z, et al. miR-34 modulates wing polyphenism in planthopper. PLoS Genet. 2019;15(6):e1008235.
53. Duursma AM, Kedde M, Schrier M, le Sage C, Agami R. miR-148 targets human DNMT3b protein coding region. RNA. 2008;14(5):872–7.
54. Tay Y, Zhang J, Thomson AM, Lim B, Rigoutsos I. MicroRNAs to Nanog, Oct4 and Sox2 coding regions modulate embryonic stem cell differentiation. Nature. 2008;455(7216):1124–8.
55. Forman JJ, Legesse-Miller A, Coller HA. A search for conserved sequences in coding regions reveals that the let-7 MicroRNA targets Dicer within its coding sequence. Proc Natl Acad Sci USA. 2008;105(39):14879–84.
56. Elcheva I, Goswami S, Noubissi FK, Spiegelman VS. CRD-BP protects the coding region of betaTrCP1 mRNA from miR-183-mediated degradation. Mol Cell. 2009;35(2):240–6.
57. Takagi S, Nakajima M, Kida K, Yamaura Y, Fukami T, Yokoi T. MicroRNAs regulate human hepatocyte nuclear factor 4alpha, modulating the expression of metabolic enzymes and cell cycle. J Biol Chem. 2010;285(7):4415–22.
58. Zhang K, Zhang X, Cai Z, Zhou J, Cao R, Zhao Y, et al. A novel class of microRNA-recognition elements that function only within open reading frames. Nat Struct Mol Biol. 2018;25(11):1019–27.
59. Gu S, Jin L, Zhang F, Sarnow P, Kay MA. Biological basis for restriction of MicroRNA targets to the 3′ untranslated region in mammalian mRNAs. Nat Struct Mol Biol. 2009;16(2):144–50.
60. Qian J, Tu R, Yuan L, Xie W. Intronic miR-932 targets the coding region of its host gene, drosophila neuroligin2. Exp Cell Res. 2016;344(2):183–93.
61. Yang J, Chen D, He Y, Meléndez A, Feng Z, Hong Q, et al. MiR-34 modulates *Caenorhabditis elegans* lifespan via repressing the autophagy gene atg9. Age (Dordr). 2013;35(1):11–22.
62. Freitas FC, Pires CV, Claudianos C, Cristino AS, Simões ZL. MicroRNA-34 directly targets pair-rule genes and cytoskeleton component in the honey bee. Sci Rep. 2017;7:40884.
63. Liu Z, Xu J, Ling L, Luo X, Yang D, Yang X, et al. miR-34 regulates larval growth and wing morphogenesis by directly modulating ecdysone signalling and cuticle protein in *Bombyx Mori*. RNA Biol. 2020;17(9):1342–51.
64. Soni K, Choudhary A, Patowary A, Singh AR, Bhatia S, Sivasubbu S, et al. miR-34 is maternally inherited in *Drosophila melanogaster* and *Danio rerio*. Nucleic Acids Res. 2013;41(8):4470–80.
65. Liu S, Li K, Gao Y, Liu X, Chen W, Ge W, et al. Antagonistic actions of juvenile hormone and 20-hydroxyecdysone within the ring gland determine developmental transitions in *Drosophila*. Proc Natl Acad Sci USA. 2018;115(1):139–44.
66. Albishi NM, Palli SR. Autophagy genes AMBRA1 and ATG8 play key roles in midgut remodeling of the yellow fever mosquito, *Aedes aegypti*. Front Insect Sci. 2023;3:1113871.

Publisher's note

Springer Nature remains neutral with regard to jurisdictional claims in published maps and institutional affiliations.